

Pb₁₂²⁻: PlumbasphereneLi-Feng Cui,^{†‡} Xin Huang,^{†‡} Lei-Ming Wang,^{†‡} Jun Li,^{*‡} and Lai-Sheng Wang^{*†‡}*Department of Physics, Washington State University, 2710 University Drive, Richland, Washington 99354, and W. R. Wiley Environmental Molecular Sciences Laboratory and Chemical Sciences Division, Pacific Northwest National Laboratory, P.O. Box 999, Richland, Washington 99352**Received: June 9, 2006; In Final Form: July 12, 2006*

Although Si or Ge is not known to form empty cage clusters such as the fullerenes, we recently found a unique 12-atom icosahedral tin cluster, Sn₁₂²⁻ (stannaspherene). Here we report photoelectron spectroscopy and theoretical evidence that Pb₁₂²⁻ is also a highly stable icosahedral cage cluster and bonded by four delocalized radial π bonds and nine delocalized on-sphere σ bonds from the 6p orbitals of the Pb atoms. Following Sn₁₂²⁻, we coin a name, plumbaspherene, for the highly stable and nearly spherical Pb₁₂²⁻ cluster, which is expected to be stable in solution and the solid state. Plumbaspherene has a diameter of ~ 6.3 Å with an empty interior volume large enough to host most transition metal atoms, affording a new class of endohedral clusters.

During recent photoelectron spectroscopy (PES) experiments aimed at understanding the semiconductor-to-metal transition in tin clusters, we found the spectra of Sn₁₂⁻ to be remarkably simple and totally different from the corresponding Ge₁₂⁻ cluster.¹ This observation led to the discovery of a C_{5v} cage structure for Sn₁₂⁻, which is only slightly distorted from the icosahedral (I_h) symmetry as a result of the Jahn–Teller effect. However, adding an electron to Sn₁₂⁻ resulted in a highly stable and closed-shell I_h Sn₁₂²⁻ cage cluster. Owing to the large 5p–5s energy separation, the I_h Sn₁₂²⁻ cage was found to be bound primarily by the 5p² electrons, which form four radial π bonds and nine in-sphere σ bonds with the 5s² electrons behaving like lone pairs. The Sn₁₂²⁻ cage was shown to be isoelectronic to the well-known B₁₂H₁₂²⁻ molecule^{2,3} with the 5s² lone pairs replacing the localized B–H bonds and was named “stannaspherene” for its π bonding characteristics and high symmetry. In this Letter, we report both experimental and theoretical evidence that the corresponding Pb₁₂²⁻ cluster also exists as a highly stable I_h cage, which has an even larger interior volume than stannaspherene and can host most transition metal atoms in the periodic table to form a new class of endohedral cage clusters.

The photoelectron spectroscopy (PES) apparatus used in the current study consists of a laser vaporization supersonic cluster beam source and a magnetic bottle electron analyzer, which have been described in detail previously.^{4,5} A disk of pure lead was used as the laser vaporization target with a helium carrier gas for the Pb₁₂⁻ experiment. Negatively charged Pb clusters (Pb_x⁻) were extracted from the cluster beam and analyzed in a time-of-flight mass spectrometer. For the Pb₁₂²⁻ experiment, a lead target containing $\sim 15\%$ potassium was used and the Pb₁₂²⁻ species was produced in the form of KPb₁₂⁻, i.e., K⁺[Pb₁₂²⁻].

* Corresponding authors. E-mail: ls.wang@pnl.gov (L.S.W.); jun.li@pnl.gov (J.L.).

[†] Washington State University.

[‡] Pacific Northwest National Laboratory.

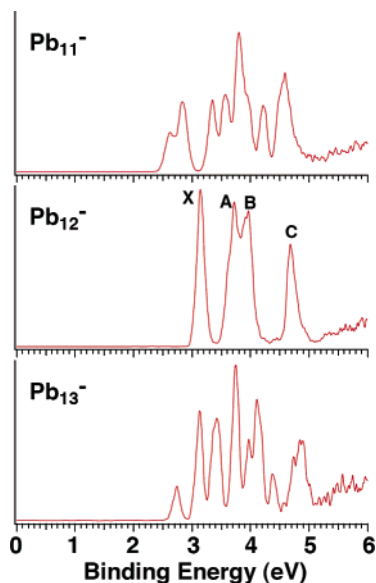


Figure 1. Photoelectron spectra of Pb_x⁻ ($x = 11–13$) at 193 nm (6.424 eV). Note the relatively simple spectral pattern of Pb₁₂⁻ with respect to those of Pb₁₁⁻ and Pb₁₃⁻.

The cluster of interest was selected and then decelerated before being photodetached by a laser beam (193 nm from an excimer laser or 266 and 355 nm from a Nd:YAG laser). Photoelectrons were analyzed by the magnetic bottle time-of-flight electron analyzer and calibrated by the known spectra of Cu⁻ and Au⁻. The PES apparatus had an electron energy resolution of $\Delta E/E \sim 2.5\%$, i.e., ~ 25 meV for 1 eV electrons.

Figure 1 displays the PES spectra of Pb_x⁻ ($x = 11–13$) at 193 nm. Clearly, the Pb₁₂⁻ spectrum is special relative to those of its neighbors, showing only four bands (X, A, B, C), whereas much more complex spectral features are observed for Pb₁₁⁻ and Pb₁₃⁻. This observation suggests that Pb₁₂⁻ should possess

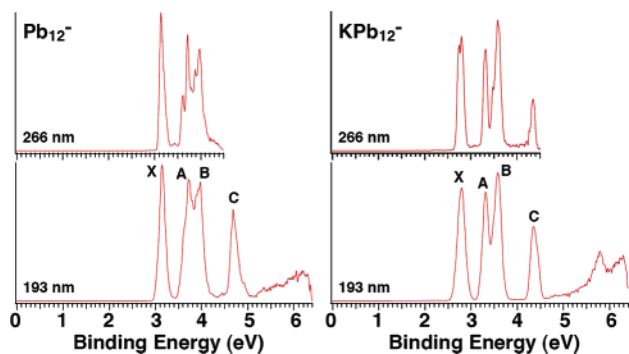


Figure 2. Photoelectron spectra of Pb_{12}^- at 266 and 193 nm compared to those of KPb_{12}^- .

a relatively high symmetry structure. We also obtained the spectrum of Pb_{12}^- at 266 nm, which is compared to the 193 nm spectrum in Figure 2, as well as to the corresponding spectra of KPb_{12}^- . The 355 nm spectrum of Pb_{12}^- (not shown) can only access the first detachment feature (X) around 3.1 eV. At 266 nm, the A and B bands of Pb_{12}^- between 3.5 and 4 eV are resolved into at least five spectral features. The spectra of KPb_{12}^- are nearly identical to those of Pb_{12}^- (Figure 2), except that they are shifted to lower binding energies due to charge transfer from K to the Pb_{12} moiety, $\text{K}^+[\text{Pb}_{12}^{2-}]$. At 266 nm, the first band (X) of KPb_{12}^- at 2.7 eV is resolved into a doublet, whereas a shoulder on the lower binding energy side is resolved in the B band at ~ 3.6 eV. The weak continuous signals beyond 5 eV in the 193 nm spectra for both Pb_{12}^- and KPb_{12}^- are due to a combination of imperfect background subtraction and possible multielectron processes (shake-up processes). The electron affinities of Pb_{12} and KPb_{12} are measured from the threshold feature to be 3.09 ± 0.03 and 2.71 ± 0.03 eV, respectively. The vertical detachment energies for the ground-state transitions for Pb_{12}^- and KPb_{12}^- are measured to be 3.14 ± 0.03 and 2.77 ± 0.03 eV, respectively. The PES spectra of Pb_{12}^- and other small Pb_x^- clusters have been measured previously at lower spectral resolution and lower photon energies.^{6,7} The current experiment yielded better resolved spectra, more accurate electron binding energies, and more spectral features to cover the valence spectral range.

Geometry optimization for Pb_{12}^- from a high-symmetry icosahedral cage led to a Jahn–Teller distorted lower symmetry C_{5v} (2A_1) species (Figure 3a),⁸ analogous to Sn_{12}^- .¹ The computed first vertical detachment energy (3.08 eV) of the C_{5v} Pb_{12}^- is in excellent agreement with the experimental value of 3.14 eV. Whereas ion mobility experiment suggests that Pb_x^+ clusters possess compact near-spherical morphologies,⁹ several theoretical studies have given various structures for neutral Pb_{12} .^{10–13} We note that the two most recent works by Wang et

al.¹² and Rajesh et al.¹³ suggested distorted cage structures for Pb_{12} . However, we find that the doubly charged Pb_{12}^{2-} species is a highly stable and perfect I_h cage with a closed electron shell (Figure 3b). We were able to synthesize Pb_{12}^{2-} stabilized by a counterion in KPb_{12}^- ($\text{K}^+[\text{Pb}_{12}^{2-}]$), which has relatively larger mass abundance than KPb_{11}^- and KPb_{13}^- . The photoelectron spectra of KPb_{12}^- are compared to those of Pb_{12}^- in Figure 2. The similarity between photoelectron spectra of KPb_{12}^- and Pb_{12}^- suggests that the Pb_{12}^{2-} cage upon K^+ coordination is probably not distorted too much from the ideal I_h symmetry, which is born out from our calculated structure (Figure 3c). Our calculations show that the K^+ counterion prefers to stay outside the cage with a C_{3v} (1A_1) symmetry, inducing very little perturbation to the Pb_{12}^{2-} cage relative to the ideal I_h symmetry. The isomer with K^+ inside the Pb_{12}^{2-} cage is much higher in energy by 2.37 eV because of the large size of the K^+ ion. The calculated vertical detachment energy (2.78 eV) of the C_{3v} KPb_{12}^- agrees very well with the experimental value of 2.77 eV, lending considerable credence to the identification of the I_h Pb_{12}^{2-} cage. In fact, we show next that the PES spectra of both Pb_{12}^- and KPb_{12}^- can be understood from the valence molecular orbitals (MOs) of the I_h Pb_{12}^{2-} , as shown in Figure 4.¹⁴

Under the I_h symmetry, the 6p-based valence orbitals of Pb transform into MOs t_{1u} , h_g , g_u , and a_g in Pb_{12}^{2-} , which form two groups with a large energy gap at the scalar relativistic level of theory (Figure 4). The 6s-based MOs are much more stable due to the so-called “inert electron pair effect” arising from the relativistic effects;¹⁵ they are separated by more than 4 eV from the 6p-based MOs and cannot be accessed even at 193 nm in our PES experiments for Pb_{12}^- and KPb_{12}^- . However, when the spin–orbit (SO) coupling effect, which is expected to be very large for Pb, is considered, the orbital pattern becomes quite different (Figure 4). The strong SO coupling transforms the MOs into three groups of energetically separated spinors: ($\epsilon_{1/2u}$, $g_{3/2g}$), ($g_{3/2u}$, $i_{5/2g}$, $e_{7/2u}$), and ($i_{5/2u}$, $e_{1/2g}$). This pattern of spinors is in remarkable qualitative agreement with the observed PES spectra for Pb_{12}^- and KPb_{12}^- , suggesting that further splittings of the MOs in the lower symmetry Pb_{12}^- and KPb_{12}^- are relatively small. This is indeed the case, as illustrated in the energy correlation diagrams in Figure 4. The small energy splitting is due to the relatively small structural distortions from the I_h structure in Pb_{12}^- and KPb_{12}^- , indicating the structural robustness of the 12 atom Pb cage.

The canonical scalar-relativistic MOs of Pb_{12}^{2-} shown in Figure 5 are similar to those of the stannaspherene Sn_{12}^{2-} ,¹ which has been shown to be valent isoelectronic to the $\text{B}_{12}\text{H}_{12}^{2-}$ molecule.^{2,3} Among the 13 valence MOs, there are four radial π orbitals (a_g and t_{1u}) and nine in-sphere σ MOs (g_u and h_g).

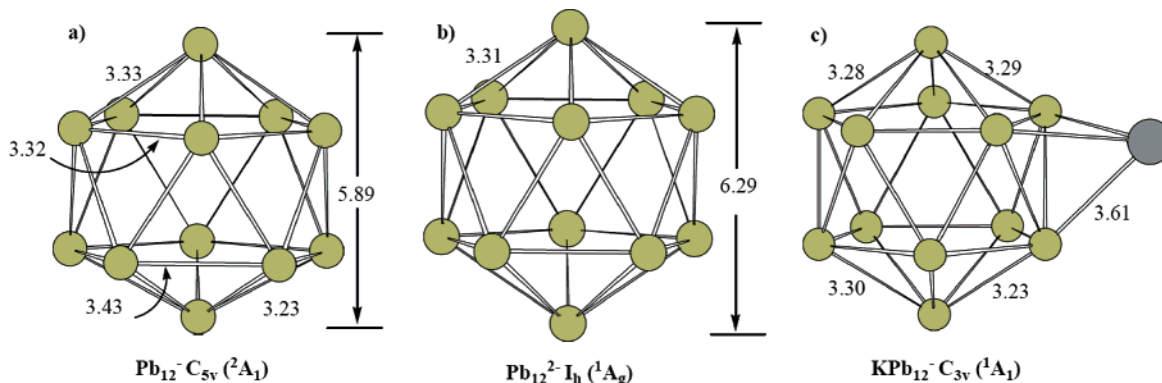


Figure 3. Optimized structures: (a) Pb_{12}^- ; (b) Pb_{12}^{2-} ; (c) KPb_{12}^- . The bond distances and cage diameters are in Å.

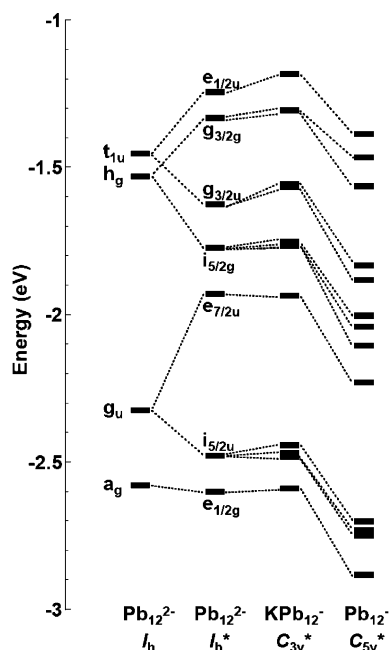


Figure 4. Scalar relativistic (SR) energy levels of the 6p-based valence molecular orbitals of the I_h Pb_{12}^{2-} and the correlation to the spin-orbit coupled levels of I_h^* Pb_{12}^{2-} and the lower symmetry C_{3v}^* $K^+[Pb_{12}^{2-}]$ and C_{5v}^* Pb_{12}^{2-} , where the asterisk indicates the double-group symmetry. The 6s-based MOs are mainly localized on each atom and are separated from the bottom of the 6p band by more than 4 eV. The energy levels of Pb_{12}^{2-} are shifted down by 2.63 eV to compare with the monoanions.

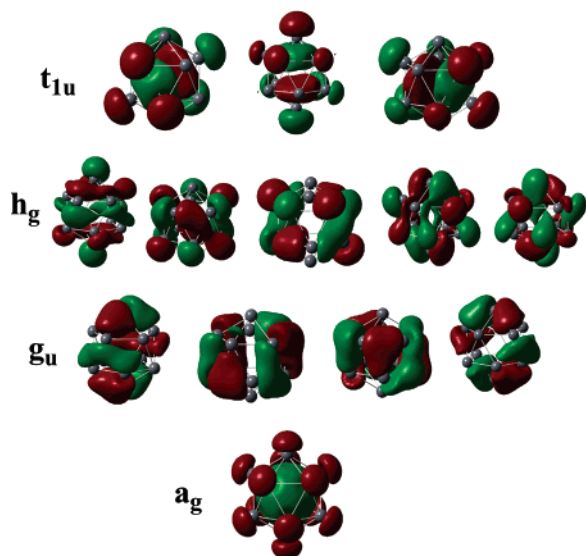


Figure 5. Contour surfaces of the valence molecular orbitals of Pb_{12}^{2-} .

Analogous to Sn_{12}^{2-} , which has been named as stannaspherene for its π bonding character and its nearly spherical structure,¹ we suggest “plumbaspherene” for the highly stable and robust Pb_{12}^{2-} cage.

Plumbaspherene has a computed diameter of 6.29 Å, slightly larger than that of stannaspherene (6.07 Å). Thus, it is expected that Pb_{12}^{2-} can trap an atom inside to form endohedral plumbaspherenes, $M@Pb_{12}$. In fact, two $M@Pb_{12}$ icosahedral cage clusters have been synthesized previously.^{16,17} A remarkable endohedral compound, $[Pt@Pb_{12}]^{2-}$, has been synthesized in solution and crystalline form with $K^+(2,2,2\text{-crypt})$ as counterions.¹⁶ X-ray diffraction and NMR experiments have confirmed that this cluster possesses I_h symmetry. It can be viewed

as a zerovalent Pt atom trapped inside plumbaspherene, $Pt@Pb_{12}^{2-}$. In a laser vaporization experiment involving Pb and Al, a cluster with the composition $AlPb_{12}^+$ was observed to be unusually intense in the mass distribution.¹⁷ Density functional calculations show that this cluster possesses an I_h structure with a closed electron shell. This cluster can be viewed as an Al^{3+} ion trapped inside plumbaspherene, $Al^{3+}@Pb_{12}^{2-}$, to give a total charge of +1. In another laser vaporization experiment involving Pb/Co, the $CoPb_{12}^-$ cluster was observed to be relatively intense in the mass distribution and was proposed to be an icosahedral $Co@Pb_{12}$ cage.¹⁸ A very recent report describes the synthesis of an empty polyhedral Pb_{10}^{2-} cage, which is compared to the $B_{10}H_{10}^{2-}$ borane.¹⁹ This result suggests that the Pb_{12}^{2-} plumbaspherene should also be a stable species in solution and can be synthesized in the condensed phase. More importantly, the current work implies that the previously observed $M@Pb_{12}$ clusters were due to the intrinsic stability of empty plumbaspherene, rather than the effect of the doped atom. Hence, we can expect that a whole new family of stable $M@Pb_{12}$ endohedral clusters may exist, analogous to the endohedral fullerenes.^{20,21} A very recent theoretical investigation on the MPb_{12}^+ and MPb_{12} ($M = B, Al, Ga, In, Tl$) clusters has provided details of the electronic structures of $M@Pb_{12}$ endohedral clusters.²²

Acknowledgment. This work was supported by the National Science Foundation (DMR-0503383) and the John Simon Guggenheim Foundation and performed at the EMSL, a national scientific user facility sponsored by DOE’s Office of Biological and Environmental Research and located at the Pacific Northwest National Laboratory (PNNL), operated for DOE by Battelle. The calculations were accomplished partially via the Molecular Science Computing Facility (MSCF) located at EMSL, PNNL.

References and Notes

- (1) Cui, L. F.; Huang, X.; Wang, L. M.; Zubarev, D. Y.; Boldyrev, A. I.; Li, J.; Wang, L. S. *J. Am. Chem. Soc.* **2006**, *128*, 8390.
- (2) Longuet-Higgins, H. C.; Roberts, M. de V. *Proc. R. Soc. A (London)* **1955**, *230*, 110.
- (3) Pitochelli, A. R.; Hawthorne, M. F. *J. Am. Chem. Soc.* **1960**, *82*, 3228.
- (4) Wang, L. S.; Wu, H. Probing the electronic structure of transition metal clusters from molecular to bulklike using photoelectron spectroscopy. In *Advances in Metal and Semiconductor Clusters. IV. Cluster Materials*; Duncan, M. A., Ed.; JAI Press: Greenwich, U.K., 1998; pp 299–343.
- (5) Wang, L. S.; Li, X. Temperature effects in anion photoelectron spectroscopy of metal clusters. In *Cluster and Nanostructure Interfaces*; Jena, P.; Khanna, S. N.; Rao, B. K., Eds.; World Scientific: Singapore, 2000; pp 293–300.
- (6) Gantefor, G.; Gausa, M.; Meiwes-Broer, K. H.; Lutz, H. O. *Z. Phys. D* **1989**, *12*, 405.
- (7) Negishi, Y.; Kawamata, H.; Nakajima, A.; Kaya, K. *J. Electron Spectrosc. Relat. Phenom.* **2000**, *106*, 117.
- (8) All structures discussed in the text were calculated using density functional theory at the hybrid B3LYP level (Becke, A. D. *J. Chem. Phys.* **1993**, *98*, 5648. Lee, C.; Yang, W.; Parr, R. G. *Phys. Rev. B* **1988**, *37*, 785). Vibrational frequencies were calculated to confirm that the structures are true minima on the potential energy surfaces. The Stuttgart quasi-relativistic pseudopotentials and basis sets were used to describe Pb and K (Fuentealba, P.; Preuss, H.; Stoll, H.; Szentpaly, L. V. *Chem. Phys. Lett.* **1982**, *89*, 418. Bergner, A.; Dolg, M.; Kuechle, W.; Stoll, H.; Preuss, H. *Mol. Phys.* **1993**, *80*, 1431), with polarization and diffuse functions added for Pb [$\zeta(d) = 0.164$, $\zeta(p) = 0.0171$]. Vertical detachment energies for the ground state transitions were calculated as the energy difference between the neutrals and anions at the anion geometries. The calculations and orbital contours were accomplished using the Gaussian 03 program and GaussView 3.0, respectively (Frisch, M. J.; et al. *Gaussian03*, revision B.04; Gaussian, Inc.: Pittsburgh, PA, 2003).
- (9) Shvartsburg A. A.; Jarrold, M. F. *Chem. Phys. Lett.* **2000**, *317*, 615.
- (10) Lai, S. K.; Hsu, P. J.; Wu, K. L.; Wu, W. K.; Iwamatsu, W. J. *Chem. Phys.* **2002**, *117*, 10715.
- (11) Doye, J. P. K.; Hendy, S. C. *Eur. Phys. J. D* **2003**, *22*, 99.

(12) Wang, B.; Zhao, J.; Chen, X.; Shi, D.; Wang, G. *Phys. Rev. A* **2005**, *71*, 033201.

(13) Rajesh, C.; Majumder, C.; Rajan, M. G. R.; Kulshreshtha, S. K. *Phys. Rev. B* **2005**, *72*, 235411.

(14) To assess the spin-orbit coupling effects in these Pb clusters, two-component relativistic DFT calculations were performed using the zero-order regular approximation (ZORA) (van Lenthe, E.; Baerends, E. J.; Snijders, J. G. *J. Chem. Phys.* **1993**, *99*, 4597) implemented in the Amsterdam Density Functional (ADF 2005.01) code [SCM, Theoretical Chemistry, Vrije Universiteit, Amsterdam, The Netherlands (<http://www.scm.com>)]. In the spin-orbit coupling calculations, the geometries were reoptimized at the scalar relativistic level using the PW91 exchange-correlation functional (Perdew, J. P.; Wang, Y. *Phys. Rev. B* **1992**, *45*, 13244) and the TZ2P Slater basis sets with the frozen core approximation to the $[1s^2-5p^6]$ core of Pb.

(15) Pyykkö, P. *Chem. Rev.* **1988**, *88*, 563.

(16) Esenturk, E. N.; Fettinger, J.; Lam, Y. F.; Eichhorn, B. *Angew. Chem., Int. Ed.* **2004**, *43*, 2132.

(17) Neukermans, S.; Janssens, E.; Chen, Z. F.; Silverans, R. E.; Schleyer, P. v. R.; Lievens, P. *Phys. Rev. Lett.* **2004**, *92*, 163401.

(18) Zhang, X.; Li, G.; Xing, X.; Zhao, X.; Tang, Z.; Gao, Z. *Rapid Commun. Mass Spectrom.* **2001**, *15*, 2399.

(19) Spiekermann, A.; Hoffmann, S. D.; Fassler, T. F. *Angew. Chem., Int. Ed.* **2006**, *45*, 3459.

(20) Chai, Y.; Guo, T.; Jin, C.; Haufler, R. E.; Chibante, L. P. F.; Fure, J.; Wang, L.; Alford, J. M.; Smalley, R. E. *J. Phys. Chem.* **1991**, *95*, 7564.

(21) Bethune, D. S.; Johnson, R. D.; Salem, J. R.; de Vries, M. S.; Yannoni, C. S. *Nature* **1993**, *366*, 123.

(22) Chen, D.-L.; Tian, W. Q.; Lu, W.-C.; Sun, C.-C. *J. Chem. Phys.* **2006**, *124*, 154313.